Available online at www.sciencedirect.com
ScienceDirect
Journal of Molecular Structure 837 (2007) 197–205
Journal of MOLECULAR STRUCTURE
www.elsevier.com/locate/molstruc

Synthesis and structural characterization of two nostoclide analogues

R.R. Teixeira [a,b], L.C.A. Barbosa [a,*], J.O. Santana [a], D.P. Veloso [b], J. Ellena [c], A.C. Doriguetto [d], M.G.B. Drew [e], F.M.D. Ismail [f]

[a] *Departamento de Química, Universidade Federal de Viçosa, Avenida P.H. Rolfs, CEP 36570-000, Viçosa, MG, Brazil*
[b] *Departamento de Química, Universidade Federal de Minas Gerais, Avenida Antônio Carlos, 6627, CEP 31270-901, Belo Horizonte, MG, Brazil*
[c] *Instituto de Física de São Carlos – USP, Cx. postal 369, CEP 13560-970, São Carlos, SP, Brazil*
[d] *Laboratório de Cristalografia, Departamento de Ciências Exatas, Universidade Federal de Alfenas, Rua Gabriel Monteiro da Silva, 714, CEP 37130-000, Alfenas, MG, Brazil*
[e] *School of Chemistry, University of Reading, Reading RG6 6AD, United Kingdom*
[f] *The Medicinal Chemistry Research Group, The School of Pharmacy and Chemistry, Liverpool John Moores University, Byrom Street, Liverpool L3 3AF, United Kingdom*

Received 6 September 2006; received in revised form 20 October 2006; accepted 21 October 2006
Available online 14 December 2006

Abstract

The vinylogous aldol reaction between appropriate aldehydes and furan-based silyloxy diene synthon generated from 3-benzyl-5*H*-furan-2-one (**3**) afforded two truncated lactone analogues [compounds (**4**) and (**5**)] of nostoclides (**2**). The compounds were fully characterized by IR, NMR (^{1}H and ^{13}C), 2D NMR spectroscopy experiments (HMBC, HSQC and NOESY), MS spectrometry and X-ray crystallography. Compounds (**4**) and (**5**) crystallized in the space group $P2_12_12_1$ and $P2_1/c$, respectively. Although expected correlations between hydrogen atoms in spatial close proximity were not observed for compound (**5**) using NMR, the stereochemistry of the exocyclic double bond of both (**4**) and (**5**) was unambiguously determined to be *Z* and *E*, respectively, using X-ray crystallography. The packing of both compounds within the crystal are stabilized by non-classical inter-molecular hydrogen bonds. DFT calculations (B3LYP/6-31+G* level) confirmed that the crystal structures possessed the lowest energies in the gas phase when compared to their geometric isomers.

Keywords: Lactones; Nostoclides; NMR analysis; X-ray; DFT

1. Introduction

A major challenge currently facing the developed world is the necessity to increase food production for supporting the current world population. To overcome this problem, it is necessary to maximize the world's agricultural efficiency, which in turns requires the control of a variety of diseases and pests among them weeds [1].

Consequently, the employment of herbicides has become the most reliable and least expensive tool for weed control throughout the world. Since the introduction of the 2,4-dichlorophenoxyacetic acid (2,4-D) in 1946 by a British research team at the Rothamsted Experimental Station, agrochemical companies have developed and brought a plethora of herbicides to the market [2]. Although important advances have been achieved in the chemical control of weeds to maximize crop production, identification and development of novel herbicides are highly desirable to fight evolution of resistance in weeds [3]. In this context, natural products may provide an economic source of new herbicides or novel lead compounds that may be optimized using known strategies [4,5].

Cyanobacterin (**1**, Fig. 1) is a phytotoxic compound isolated from the blue-green alga *Scytonema hofmanni* [6]. It is toxic to most cyanobacteria at a concentration of 5 μM and also inhibits the growth of most eukaryotic algae and

* Corresponding author. Tel.: +55 31 3899 3068; fax: +55 31 3899 3065.
E-mail address: lcab@ufv.br (L.C.A. Barbosa).

0022-2860/$ - see front matter © 2006 Elsevier B.V. All rights reserved.
doi:10.1016/j.molstruc.2006.10.014

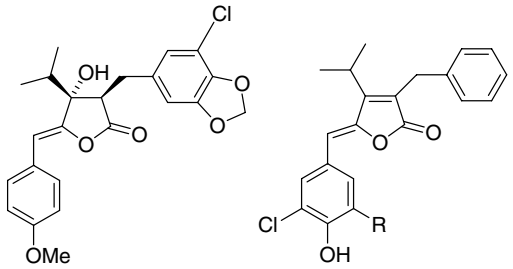

Fig. 1. Structures of cyanobacterin and nostoclides.

several monocotyledonous and dicotyledonous angiosperms [7,8]. Cyanobacterin acts by inhibiting photosynthetic electron transport in isolated chloroplasts in a similar way to the herbicide 3-(3,4-diclorophenyl)-1,1-dimethylurea [9], leading to a cascade of events which result in the disruption of the thylakoid membrane [10].

Although several studies have been carried out on the mode of action of cyanobacterin, the biological activity of the structurally similar natural lactones, know as nostoclides I and II (Fig. 1: **2a** and **2b**), produced by a cyanobacterium (or blue-green alga; *Nostoc* sp.) symbiont partner within *Peltigera canina*, has not yet been fully investigated. Nostoclides I and II have been shown to possess moderate cytotoxicity against the mouse neuroblastoma cell lines Neuro-2a CCL and KB CCL 17 [11]. Owing to the structural similarity of nostoclides and cyanobacterin (both compounds have in common the presence of a 3-benzyl-5-benzylidene-4-isopropyl-dihydro-furan-2-one ring system) and the fact that *P. canina* cultures are usually not contaminated with microorganisms, it has been suggested that these chlorinated compounds may be alleopathic agents.

The presence of chlorine, which is relatively rare compared to bromine but more abundant than fluorine within natural products, a property exploited in many herbicides, probably improves uptake of this compound into target organisms [12].

As part of a continuous effort to develop new herbicides in our laboratory [13], we decided to investigate the potential phytotoxicity of nostoclide analogues. Herein, we report the preparation of two lactones analogues to nostoclides. The lactones were fully characterized by spectral and spectrometric analyses as well as single crystal X-ray diffraction techniques. It was important to establish the molecular geometry since it is required for constructing structure–activity relationships and, indirectly, spatial requirements of the receptors at which these compounds act.

2. Experimental

2.1. Material and methods

All reactions were carried out under a protective atmosphere of dry nitrogen. Dichloromethane and diisopropylethylamine (DIPEA) were dried prior to use; dichloromethane was distilled over calcium hydride; diisopropylethylamine was distilled over potassium hydroxide. Commercially *tert*-butyldimethylsilyl trifluoromethanesulfonate (TBDMSOTf), piperonal, 2,4,6-trimethoxy benzaldehyde and 8-diazabyciclo[5.4.0]undec-7-ene (DBU) were utilized without further purification. The ^{1}H and ^{13}C NMR spectra were recorded on *Brucker AVANCE DRX* 400 spectrometer at 400 and 100 MHz, respectively, using $CDCl_3$ as solvent and TMS as internal standard. Mass spectra were obtained on SHIMADZU GCMS-QP5050A instrument by direct injection (DI temperature program: 40 °C/min until temperature reaches 60 °C; then 80 °C/min until temperature reaches 300 °C; detector temp: 280 °C). IR spectra were taken from Perkin-Elmer Paragon 1000 FTIR spectrophotometer. Melting points are uncorrected and were obtained from MQAPF-301 melting point apparatus (Microquimica, Brazil). Analytical thin-layer chromatography was conducted on SILICYCLE aluminum backed TLC. Column chromatography was performed over ULTRACHEM silica gel (200–400 mesh).

2.2. Synthesis of 5(*Z*)-3-benzyl-5-(1,3-dioxalanebenzilidene)-5H-furan-2-one (**4**)

To a two neck round-bottomed flask, under nitrogen atmosphere, were added 3-benzyl-5*H*-furan-2-one (**3**) (106 mg; 0.61 mmol), 3 mL of anhydrous dichloromethane, *tert*-butyldimethylsilyl trifluoromethanesulfonate (170 μL; 0.74 mmol), diisopropylethylamine (310 μL; 1.2 mmol) and piperonal (180 mg; 1.2 mmol). The resulting mixture was stirred at room temperature for 1 h. After adding DBU (120 μL; 1.22 mmol), the reaction mixture was refluxed for an additional 3 h and 70 mL of dichloromethane was added. The resulting organic layer was washed with 3 mol/L HCl aqueous solution (2× 25 mL) and brine (25 mL). After separation, the organic layer was dried over $MgSO_4$, filtered, and concentrated under reduced pressure. The resulting material was purified by column chromatography on silica gel eluted with hexane–diethyl ether (6:1). Since, some fractions revealed the presence of impurities, after they were combined and evaporated, the resulting solid was recrystallized from a mixture of hexane–dichloromethane. Compound (**4**) was obtained as pale yellow crystals in 83% yield (155 mg, 0.51 mmol).

Mp = 181.1–181.8 °C; $R_f = 0.28$ (hexano–dichloromethane, 1:1); IR (KBr, $\overline{\nu}_{max}/cm^{-1}$): 3108, 3055, 3025, 2892, 1736, 1654, 1600, 1489, 1446, 1379, 1341, 1262, 1036, 935; RMN de ^{1}H (400 MHz, $CDCl_3$) δ (J/Hz): 3.71 (s, 2H; H-6), 5.78 (s, 1H; H-5), 5.98 (s, 2H; -O–CH_2–O-), 6.79 (d, 1H, $J_{3'',2''} = 8.2$; H-3″), 6.91 (s, 1H; H-3), 7.10 (dd, $J_{2'',3''} = 8.2$, $J_{2'',6''} = 1.3$; 1H, H-2″), 7.25–7.36 (m, 5H; H-2′a H-6′), 7.42 (d, 1H, $J_{6'',2''} = 1.3$; H-6″). RMN de ^{13}C (100 MHz, $CDCl_3$) δ: 31.68 (C-6), 101.47 (-O–CH_2–O-), 108.56 (C-3″), 109.94 (C-6″), 112.66 (C-5), 125.74 (C-2″), 126.92 (C-4′), 127.51 (C-1″), 128.84 (C-3′/C-5′), 128.93 (C-2′/C-6′), 131.56 (C-2), 137.36 (C-1′),

139.60 (C-3), 146.24 (C-4), 148.42 (C-4″)*, 148.26 (C-5″)*, 170.42 (C-1); EM, *m/z* (%): 306, $C_{19}H_{14}O_4$, [M^+], (100); 261 (4.2); 231 (7.7), 203 (7.5), 162 (32.0), 153 (7.0), 134 (33.7), 115 (22.3), 104 (16.7), 101 (18.3), 91 (12.6), 77 (8.9), 76 (41.2), 65 (7.7), 51 (11.1). *The assignments could be reversed.

2.3. Synthesis of 5(*E*)-3-benzyl-5-(2,4,6-trimetoxibenzilidene)-5*H*-furan-2-one (**5**)

To a two neck round-bottom flask, under nitrogen atmosphere, were added 3-benzyl-5*H*-furan-2-one (**3**) (106 mg; 0.61 mmol), 3 mL of anhydrous dichloromethane, *tert*-butyldimethylsilyl trifluoromethanesulfonate (170 μL; 0.74 mmol), diisopropylethylamine (310 μL; 1.2 mmol) and 2,4,6-trimethoxy benzaldehyde (146 mg; 0.74 mmol). The resulting mixture was stirred at room temperature for 1 h. After DBU (120 μL; 1.22 mmol) was added, the reaction mixture was refluxed for additional 3 h and 70 mL of dichloromethane was added. The resulting organic layer was washed with 3 mol/L HCl aqueous solution (2× 25 mL) and brine (25 mL). Subsequently, the organic layer was separated, dried over $MgSO_4$, filtered, and concentrated under reduced pressure. The resulting material was purified by column chromatography on silica gel eluted with hexane–ethyl acetate (4:1). The procedure described afforded compound (**5**) (184 mg, 0.52 mmol, 86% yield) as a yellow solid. Yellow crystals suitable for X-ray analysis were obtained from a mixture of hexane–dichloromethane.

Mp = 107.9–109.0 °C; $R_f = 0.29$ (hexano–EtOAc, 4:1); IV (KBr, $\bar{\nu}_{max}/cm^{-1}$): 3001, 2938, 2840, 1747, 1602, 1583, 1495, 1469, 1455, 1229, 1119, 953, 814, 701; RMN de ^1H (400 MHz, $CDCl_3$) δ (*J*/Hz): 3.68 (s, H-6; 2 H); 3,72 (s, 2″/6″-OCH_3; 6H); 3.82 (s, 4″-OCH_3; 3H); 6.10 (s, H-3″/H-5″; 2H); 6.54 (s, H-5; 1H); 7.05 (s, H-3; 1H); 7.22–7.33 (m, H-2′a H-6′, 5H); RMN de ^{13}C (100 MHz, $CDCl_3$) δ: 31.82 (C-6); 55.42 (4″-OCH_3); 55.57 (2″/6″-OCH_3); 90.74 (C-3″/C-5″); 103.82 (C-1″); 105.65 (C-5); 126.72 (C-4′); 128.67 (C-3′/C-5′); 128.96 (C-2′/C-6′); 132.92 (C-2); 137.77 (C-1′); 137.85 (C-3); 148.70 (C-4); 158.71 (C-2″/C-6″); 161.89 (C-4″); 170.25 (C-1); EM, *m/z* (%): 352, $C_{21}H_{20}O_5$ [M^+], (100); 281 (7.4); 208 (7.8); 193 (11.4); 181 (15.0); 166 (26.5); 138 (23.3); 115 (16.3); 91 (19.1); 77 (9.8); 76 (5.0); 69 (11.8); 65 (8.5); 51 (6.1) Da.

2.4. Single crystal X-ray diffraction studies

Suitably sized crystals of both (**4**) and (**5**) were selected for single crystal X-ray diffraction experiments. Low temperature (150 K) X-ray diffraction data collections were performed on an Enraf–Nonius Kappa-CCD diffractometer using graphite–monochromated MoKα radiation (0.71073 Å). Data were collected up to 50° in 2θ, with a redundancy of 4 for both compounds. The final unit cell parameters were based on all reflections. Data collections were performed using the COLLECT program [14]; integration and scaling of the reflections were performed with the HKL Denzo-Scalepack system of programs [15]. The structure was solved by direct methods with SHELXS-97 [16]. The model was refined by full-matrix least-squares on F^2 with SHELXL-97 [17]. All hydrogen atoms were stereochemically positioned and refined with the SHELXL-97 riding model. Hydrogen atoms were refined with C–H distances of 0.93–0.97 Å and were set isotropic with a thermal parameter 20% greater than the equivalent isotropic displacement parameter of the atom to which they were bonded. This percentage was set to 50% for the hydrogen atoms of the CH_3 groups.

In spite of compound (**4**) crystallizing in a non-centrosymmetric space group, the Flack parameter was not refined during X-ray crystallographic analysis. Given that in this case the most electron-rich atom is oxygen, which does not have an anomalous scattering large enough (using MoK_α radiation) to permit determination of the absolute structure using X-ray diffraction, Friedel pairs were averaged before refinement.

Data collections and experimental details for (**4**) and (**5**) are summarized in Table 1. The programs WinGX [18] and enCIFer [19] were used to prepare materials for publication. The programs MERCURY [20] and ORTEP-3 [21] were used to generate the molecular graphics.

Table 1
Crystal data and structure refinement for compounds (**4**) and (**5**)

	(**4**)	(**5**)
Empirical formula	$C_{19}H_{14}O_4$	$C_{21}H_{20}O_5$
Formula weight	306.30	352.37
Crystal system	Orthorhombic	Monoclinic
Space group	$P2_12_12_1$	$P2_1/c$
Unit cell dimensions	$a = 6.7188(4)$ Å $b = 12.6624(5)$ Å $c = 17.3713(12)$ Å $\alpha = \beta = \gamma = 90°$	$a = 6.861(5)$ Å $b = 13.758(5)$ Å $c = 19.351(5)$ Å $\alpha = \gamma = 90°$; $\beta = 106.03(2)°$
Volume (Å^3)	1477.88(15)	1755.6(15)
Z	4	4
Density – calculated	1.377 mg/m^3	1.333
Absorption coefficient	0.097 mm^{-1}	0.095
F(000)	640	744
Crystal size	$0.08 \times 0.10 \times 0.30$ mm^3	$0.12 \times 0.15 \times 0.22$ mm^3
θ-Maximum	27.87°	25.00°
Reflections collected	3493	3056
Independent reflections	2009 [R(int) = 0.0248]	3056 [R(int) = 0.0534]
Completeness (%)	98.6	98.8
Data/restraints/parameters	2009/0/209	3056/0/236
Goodness-of-fit on F^2	1.068	1.124
Final *R* indices [$I > 2\sigma(I)$]	$R_1 = 0.0399$, w$R_2 = 0.1027$	$R_1 = 0.1131$, w$R_2 = 0.3214$
R indices (all data)	$R_1 = 0.0479$, w$R_2 = 0.1081$	$R_1 = 0.1535$, w$R_2 = 0.3456$
Largest diff. peak and hole	0.148 and −0.176 e·Å^{-3}	0.599 and −0.343 e·Å^{-3}

2.5. DFT calculations

Structures were built using the Cerius software package [22] and approximate structures were obtained using molecular mechanics minimisation. The structures were then geometry optimised at the B3LYP/6-31+G* level using the GAUSSIAN03 program [23].

3. Results and discussion

Compounds (**4**) and (**5**) were constructed using the vinologous aldol reaction with the silyloxy diene furan synthon and the relevant aldehyde [24]. Thus, reaction of lactone (**3**), prepared as shown in Fig. 2, with the corresponding aldehydes in the presence of *tert*-butyldimethylsilyl trifluoromethanesulfonate and diisopropylethylamine followed by treatment of the silyl ether generated *in situ* with DBU afforded the compounds (**4**) and (**5**) in good yields.

Compounds (**4**) and (**5**) were fully characterized based on NMR, IR, MS and X-ray diffraction (XRD) analyses. The mass spectrum of lactones (**4**) and (**5**) revealed mass ions, respectively, at *m*/*z* 306 and 352 Da which correlated with the respective molecular formulae $C_{19}H_{14}O_4$ for compound (**4**) and $C_{21}H_{20}O_5$ for compound (**5**), respectively.

IR absorption bands at 1736 cm^{-1} [compound (**4**)] and 1732 [compound (**5**)], corresponding to the carbonyl stretching of the unsaturated lactones, were observed. The two bands at 1261 and 935 cm^{-1} observed in the IR spectrum of (**4**) are associated with the 1,3-dioxalane group. The ^1H and ^{13}C NMR assignments for compounds (**4**) and (**5**) are summarized in Table 2.

The ^1H NMR spectrum of (**4**) contained three signals at δ_H 6.79 (d, $J = 8.2$, 1H; H-3″), δ_H 7.10 (dd, $J = 8.2$ and 1.3, 1H; H-2″) and δ_H 7.42 (d, $J = 1.3$, 1H; H-6″) characteristics of 1,3,4-substituted aromatic rings. These signals were correlated with the corresponding carbons via HSQC experiment. Thus, the signals at δ_C 108.56, 109.94 and 125.74 were assigned, respectively to C-3″, C-6″and C-2″. The signal observed at δ_H 3.71 (s, 2H) was unequivocally attributed to the methylene hydrogens of the benzyl group while the signal at δ_C 31.68 could be assigned to the benzylic carbon. The olefinic hydrogens of (**4**) showed chemical shifts at δ_H 5.78 (s, 1H; H-5) and δ_H 6.91 (s, 1H; H-3). The assignments were possible based on the information provided by the HMBC experiment. In the contour plot it was noticed long range correlations between H-3 and carbons C-1 and C-6. Correlations of this nature were also observed between H-5 and carbons C-2″ and C-6″.

Once the signals related to H-3 and H-5 were identified, it was possible to assign the signals to carbons C-3 (δ_C 139.60) and C-5 (δ_C 112.66) through HSQC experiment. The remaining assignments were possible based on the information provided by HMBC and HSQC experiments. For example, the long range correlations observed between the signal at δ_C 146.24 and hydrogens H-3 and H-5 suggested association to C-4. The signal at δ_C 131.56 was assigned to C-2 based on the long range connectivity of this signal with H-3 and H-6. The HMBC contour plot also revealed a correlation between the signal at δ_C 127.51 and H-2″, H-6″ and H-3″ allowing assignment of this signal to C-1″. The

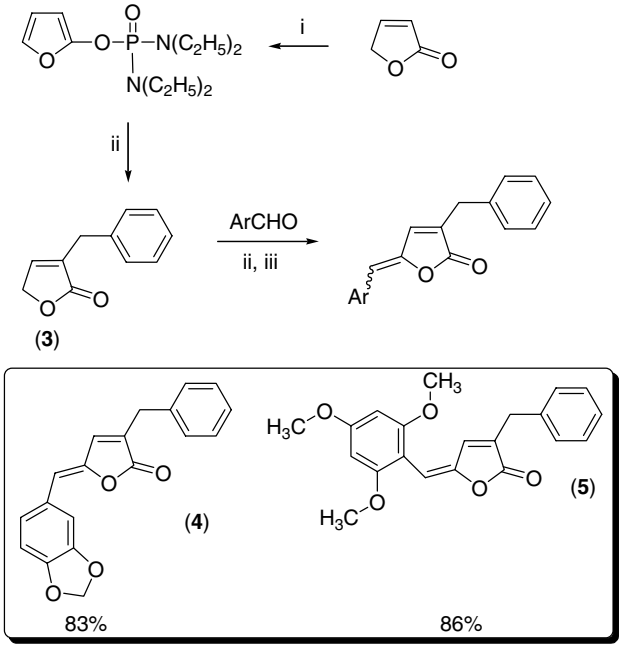

Fig. 2. Reagents and conditions employed to prepare (**4**) and (**5**) where: (i) $POCl_3$/*i*-Pr_2EtN; Me_2NH (51%); (ii) *n*-BuLi, THF, −78 °C (1 h); $PhCH_2Br$ (−78 °C → rt); HCOOH (45 min) (67% overall yield); (iii) TBDMSOTf, DIPEA, CH_2Cl_2, rt, 1 h; DBU, reflux, 3 h.

Table 2
^1H and ^{13}C NMR data of compounds (**4**) and (**5**) using $CDCl_3$ as solvent and TMS as internal standard (δ in ppm and coupling constants J in Hz) where mult, multiplicity

Position	**4**		**5**	
	δ_C	δ_H(mult., J)	δ_C	δ_H(mult., J)
1	170.42		170.25	
2	131.56		132.92	
3	139.60	6.91 (s)	137.85	7.05 (s)
4	146.24		148.70	
5	112.66	5.78 (s)	105.65	6.54 (s)
6	31.68	3.71 (s)	31.82	3.68 (s)
1′	137.36		137.77	
2′, 6′	128.93	7.25–7.36 (m)	128.96	7.22–7.33 (m)
3′, 5′	128.84	7.25–7.36 (m)	128.67	7.22–7.33 (m)
4′	126.92	7.25–7.36 (m)	126.72	7.22–7.33 (m)
1″	127.51		103.82	
2″	125.74	7,10 (dd, 8.2 and 1.3)	158.71	
3″	108.56	6.79 (d, 8.2)	90.74	6.10 (s)
4″	148.42[a]		161.89	
5″	148.26[a]		90.74	6.10 (s)
6″	109.94	7.42 (d, 1.3)	158.71	
-O–CH_2–O-	101.47	5.98 (s)		
4″-OCH_3			55.42	3.82 (s)
2″/6″-OCH_3			55.57	3.72 (s)

[a] The assignments could be reversed.

signals at δ_C 137.61; 128.97; 128.84 and 126.92 were assigned to the aromatic carbons of benzylic moiety and specific attributions are shown in Table 2. The HSQC experiment revealed correlations between these signals and the multiplet at δ_H 7.25–7.36. Finally, the signals at δ_C 148.42/148.26 were related to carbons C-4″/C-5″. A correlation between hydrogens H-3 and H-5, observed in NOESY experiment, demonstrated that the exocyclic double bond presented a *Z* configuration. Other correlations observed in the NOESY contour plot are illustrated in Fig. 3. The stereochemistry of the double bond of (**4**) was unambiguously determined by X-ray crystallography (Fig. 4).

The lactone (**4**) is almost flat (with the least-square plane passing through rings A, C and D) with phenyl ring B adopting an angle of 74.32(5)° (Fig. 4). The main geometric parameters of (**4**) are given in Table 3. All atoms in the rings A, C and D, including C5, C6, and O1, lie within −0.187(2) Å of the least-squares plane through the three-ring system (Rms deviation of fitted atoms = 0.0595 Å). The structural features responsible for maintaining coplanarity is conjugation between the rings A and C (unsaturated C4–C5 bond) and the weak non-classical intra-molecular hydrogen bond involving C18–H18…O2 (see Table 4). As expected, the phenyl ring B is planar (Rms deviation of fitted atoms = 0.0033 Å). The molecular conformation of (**4**), analyzed using the MOGUL [25], a knowledge base of molecular geometry derived from the Cambridge Structural Database (CSD) [26] that provides rapid access to information on the preferred values of bond lengths, valence angles and acyclic torsion angles, indicated that all bond lengths and bond angles are in agreement with the expected values.

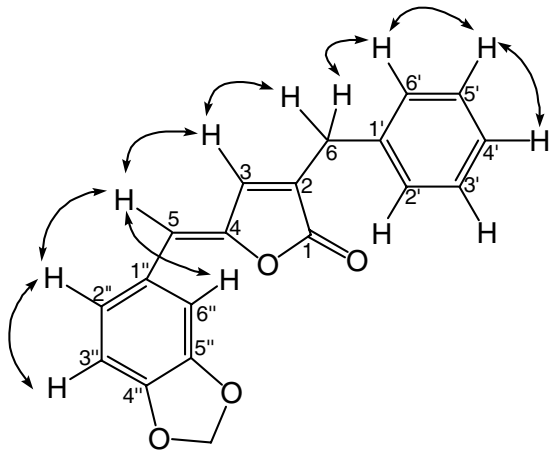

Fig. 3. Correlations observed for compound (**4**) in the NOESY experiment.

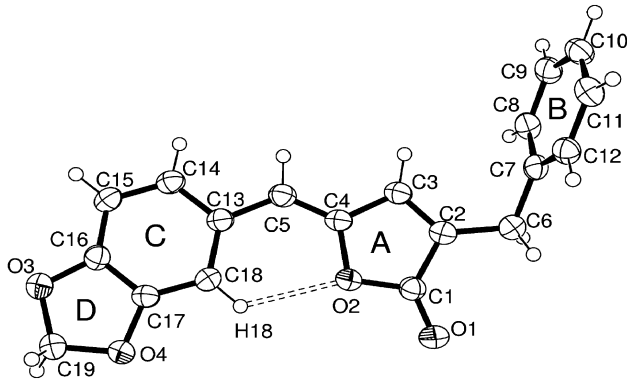

Fig. 4. ORTEP-3 view of the lactone (**4**) showing the ring and atom labelling and 50% probability ellipsoids. H atoms are shown as spheres of arbitrary radii.

The lactone (**4**) exhibits five weak non-classical inter-molecular hydrogen bonds (see Figs. 5 and 6 and Table 4). Three inter-molecular hydrogen bonds involving C15—H15 ⋯ O4^{i}, C5-H5…O1^{i} and C3–H3 ⋯ O1^{i} (symmetry code: (i) = $x-1$, y, z) give rise to an infinite one-dimensional chain parallel to the [100] direction (Fig. 5). It is important to emphasize that either the C5–H5 or C3–H3 groups act as an intermolecular H bond donor to the O1, forming a bifurcated H bond. The chains form a planar network, connected by two other weak inter-molecular hydrogen bonds: C19^{iv}–H19b^{iv} ⋯ O1 and C11–H11 ⋯ O2^{vi} (symmetry codes: (iv) = $-x+1/2$, $-y+2$, $z+1/2$; (vi) = $-x+1$, $y-1/2$, $-z+3/2$). Therefore, the individual chains are linked to one another, forming an infinite two-dimensional network parallel to the (011) plane. Double chains, stabilized by van der Waals (VDW) interactions, are formed along [100] direction. The double chains are related by 2_1 screw axis symmetry along [100] and the distance between each individual chain is ~3.3 Å as shown in Fig. 6. Comparing Figs. 5 and 6 is that O1 atom reveal an interesting trifurcated H bonding motif: C5^{ii}–H5^{ii} ⋯ O1, C3^{ii}–H3^{ii} ⋯ O1, and C19^{iv}–H19b^{iv} ⋯ O1 (symmetry code: (ii) = $x+1$, y, z; (iv) = $-x+1/2$, $-y+2$, $z+1/2$). The angles between H5^{ii} ⋯ O1 ⋯ H3^{ii}, H5^{ii} ⋯ O1 ⋯ H19b^{iv}, and H3^{ii} ⋯ O1 ⋯ H19b^{iv} are 62.03°, 80.45°, and 68.52°, respectively.

Information provided by ^{1}H and ^{13}C NMR analyses along with the data furnished by HMBC and HSQC experiments were also crucial to the characterization of lactone (**5**). Specific assignments obtained for hydrogen and carbon atoms are provided in Table 2. Inexplicably, the attempt to determine the stereochemistry of the exocyclic double bond based on NOESY experiment failed and anticipated correlations between hydrogens in spatial close proximity were not observed. Single crystal X-ray diffraction of (**5**), in the solid state, revealed that it presents an *E* configuration (Fig. 7). The ORTEP-3 view of the lactone (**5**) shows that this compound is also almost flat excluding the phenyl ring B, as observed for lactone (**4**). The main structural features responsible for the coplanarity and the conjugation between the rings A and C is the unsaturated C4–C5 bond and two weak non-classical intra-molecular hydrogen bonds involving, in this case, C3–H3…O3 and C5–H5…O5 (see Table 6). The least-squares plane through the planar phenyl ring B (Rms deviation of fitted atoms = 0.0056 Å) forms an angle of 77.7(2)° with the least-square plane (Rms deviation of fitted

Table 3
Bond lengths (Å) and angles (°) for lactone (**4**) determined by XRD (query value) and MOGUL (Mogul value) intra-molecular analysis

Fragment	Query value	Mogul value	Fragment	Query value	Mogul value
C(1)–O(1)	1.213(3)	1.21(2)	C(19)–O(4)	1.431(3)	1.43(2)
C(1)–O(2)	1.384(2)	1.39(2)	C(19)–O(3)	1.434(3)	1.43(2)
C(1)–C(2)	1.462(3)	1.47(3)	C–$C_{ring\ B}$	1.390(5)	1.38(3)
C(2)–C(3)	1.341(3)	1.36(3)			
C(2)–C(6)	1.503(3)	1.51(3)	C–C–$C_{Ring\ B}$	120(1)	120(2)
C(3)–C(4)	1.439(3)	1.43(2)	C–C–$C_{Ring\ C}$	120(3)	120(3)
C(4)–C(5)	1.345(3)	1.3(1)	O(2)–C(1)–C(2)	108.6(2)	108[a]
C(4)–O(2)	1.400(2)	1.38(2)	C(3)–C(2)–C(1)	106.8(2)	No hits
C(5)–C(13)	1.455(3)	1.47(2)	C(2)–C(3)–C(4)	109.5(2)	No hits
C(6)–C(7)	1.502(3)	1.51(2)	O(2)–C(4)–C(3)	107.7(2)	108(1)
C(13)–C(14)	1.401(3)	1.39(2)	C(4)–C(5)–C(13)	131.1(2)	132(7)
C(13)–C(18)	1.413(3)	1.40(2)	C(7)–C(6)–C(2)	112.8(2)	113(2)
C(14)–C(15)	1.395(3)	1.38(2)	O(3)–C(16)–C(17)	110.2(2)	110(1)
C(15)–C(16)	1.376(3)	1.39(2)	O(4)–C(17)–C(16)	109.7(2)	110(1)
C(16)–O(3)	1.371(2)	1.38(2)	O(4)–C(19)–O(3)	107.9(2)	108(2)
C(16)–C(17)	1.381(3)	1.39(3)	C(1)–O(2)–C(4)	107.4(2)	107(1)
C(17)–O(4)	1.370(2)	1.38(2)	C(16)–O(3)–C(19)	105.7(2)	105(2)
C(17)–C(18)	1.375(3)	1.38(2)	C(17)–O(4)–C(19)	106.0(2)	105(2)

[a] One hit appeared in the MOGUL intra-molecular analysis.

Table 4
Hydrogen bonding for lactone (**4**)

D—H···A[a]	*D*–H (Å)	H···A (Å)	*D*···A (Å)	*D*–H···A (°)
C19–H18…O2	0.93	2.414	3.021(2)	123
C3–H3···O1^{i}	0.93	2.611	3.333(2)	135
C5–H5···O1^{i}	0.93	2.490	3.333(2)	151
C15–H15···O4^{i}	0.93	2.470	3.332(2)	155
C19^{iv}–H19b^{iv}···O1	0.97	2.510	3.452(3)	164
C11–H11···O2^{vi}	0.93	2.666	3.370(3)	133

[a] Symmetry codes: i = $x-1$, y, z; iv = $-x+1/2$, $-y+2$, $z+1/2$; vi = $-x+1$, $y-1/2$, $-z+3/2$.

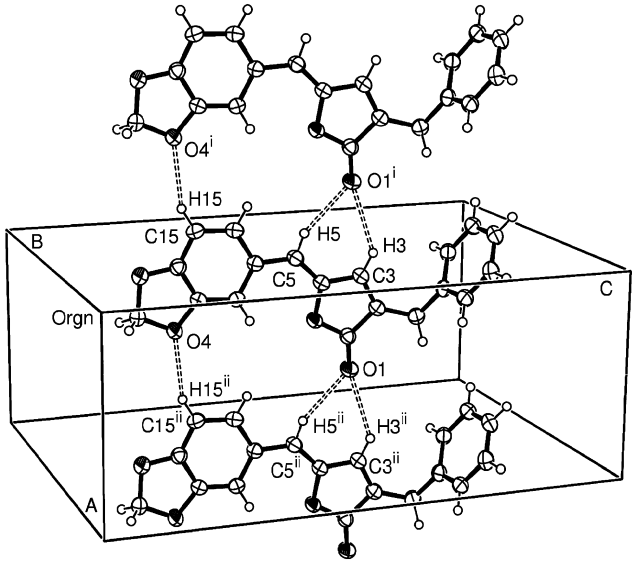

Fig. 5. View of the network of hydrogen bonds parallel to [001] which stabilizes the packing of (**4**). *Symmetry codes*: i = $x-1$, y, z; ii = $x+1$, y, z.

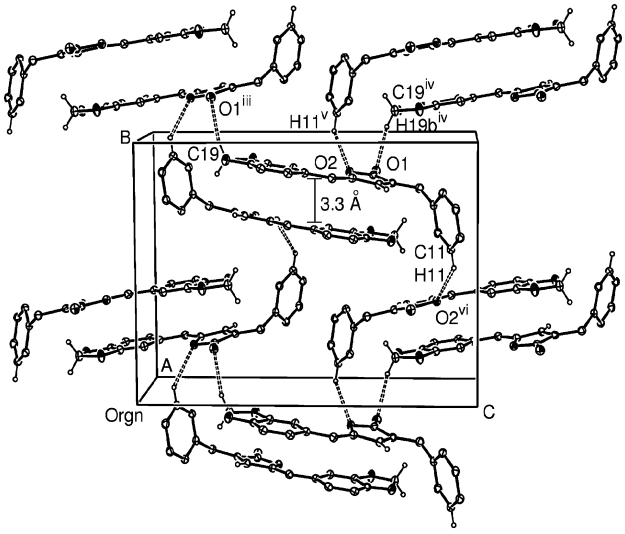

Fig. 6. The crystal structure of (**4**) projected onto the bc plane (011). Symmetry codes: iii = $-x+1/2$, $-y+2$, $z-1/2$; iv = $-x+1/2$, $-y+2$, $z+1/2$; v = $-x+1$, $y+1/2$, $-z+3/2$; vi = $-x+1$, $y-1/2$, $-z+3/2$.

atoms = 0.0323 Å) passing through the remaining atoms. Their main geometric experimental parameters and its MOGUL analysis are given in Table 5.

The crystal packing of (**5**) is also stabilized by weak non-classical hydrogen bonds (Fig. 8 and Table 6). A dimeric chain is formed along [010] linked by bifurcated

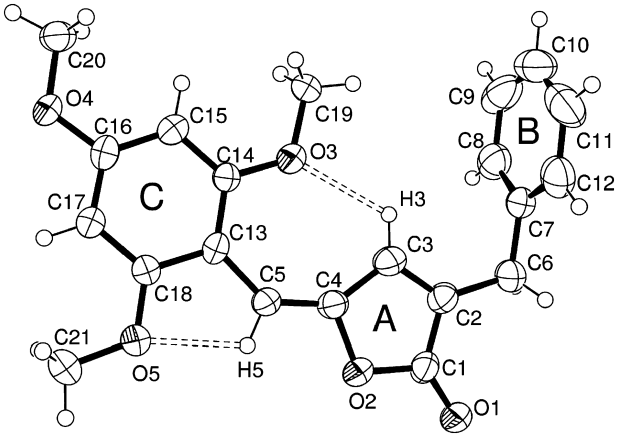

Fig. 7. ORTEP-3 view of the lactone (**5**), showing the ring and atom labelling and 50% probability ellipsoids and H atoms are shown as spheres of arbitrary radii.

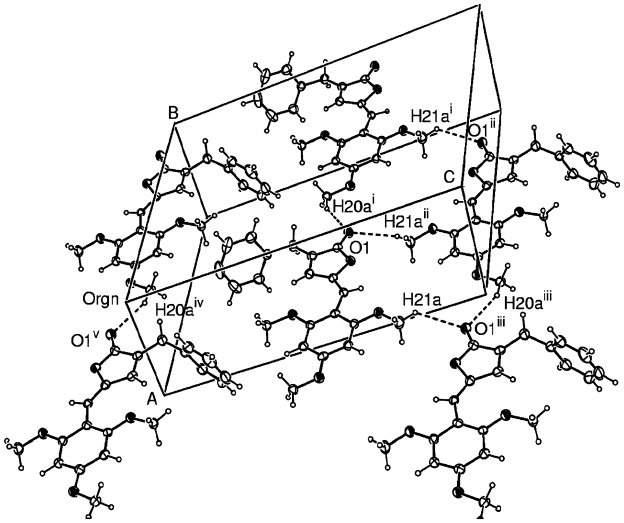

Fig. 8. View of the network of hydrogen bonds parallel to [010] for compound (**5**). Symmetry codes: i = x, $y+1$, z; ii = $-x+2$, $y+1/2$, $-z+3/2$; iii = $-x+2$, $y-1/2$, $-z+3/2$; iv = $-x+1$, $y+1/2$, $-z+1/2$; v = $-x+1$, $y-1/2$, $-z+1/2$.

inter-molecular hydrogen bonds: C20–H20a^{i}…O1 and C21–H21a^{ii}…O1 (symmetry code: i = x, $y+1$, z; ii = $-x+2$, $y+1/2$, $-z+3/2$). As in (**4**) The dimeric chains are associated with one another by van der Waals and H…π-aryl interactions along [101], forming an infinite two-dimensional network parallel to the (10-1) plane. The planes are also linked to one another by four very weak non-classical hydrogen bonds (C20–H20b…O2^{vi}, C20–H20c…O2^{vii}, C19–H19c…O2^{vi}, C19–H19b…O5^{vii} where vi = $-x+2$, $-y$, $-z+1$; vii = $-x+1$, $-y$, $-z+1$), as shown in Fig. 9. The resulting is an extended three-dimensional supramolecular assembly mediated mainly by C–H…O bonding.

In order to ascertain if the predicted stability of the various possible geometric isomers of (**4**) and (**5**), was kinetic

Table 6
Hydrogen bonding for lactone (**5**)

D–H…A[a]	D–H (Å)	H…A (Å)	D…A (Å)	D–H…A (°)
C3–H3…O3	0.93	2.253	2.839	120
C5–H5…O5	0.93	2.179	2.660	111
C19–H19c…O5^{vi}	0.96	2.945	3.742	141
C19–H19b…O5^{vii}	0.96	2.819	3.595	139
C20–H20a…O1^{viii}	0.96	2.525	3.401	152
C20–H20b…O2^{vi}	0.96	2.776	3.676	156
C20–H20c…O2^{vii}	0.96	2.794	3.701	158
C21–H21a…O1^{iii}	0.96	2.652	3.358	131

[a] Symmetry codes: iii = $-x+2$, $y-1/2$, $-z+3/2$; vi = $-x+2$, $-y$, $-z+1$; vii = $-x+1$, $-y$, $-z+1$; viii = x, $y-1$, z.

Table 5
Bond lengths (Å) and angles (°) for lactone (**5**) determined by XRD (Query value) and MOGUL (Mogul value) intra-molecular analysis

Fragment	Query value	Mogul Value	Fragment	Query value	Mogul value
C(1)–O(1)	1.213(7)	1.21(2)	C(19)–O(3)	1.445(6)	1.42(4)
C(1)–O(2)	1.373(7)	1.39(2)	C(20)–O(4)	1.428(7)	1.42(4)
C(1)–C(2)	1.433(9)	1.47(3)	C–$C_{ring\ B}$	1.374(21)	1.38(3)
C(2)–C(3)	1.331(8)	1.36(3)			
C(2)–C(6)	1.505(9)	1.51(3)	C–C–$C_{Ring\ B}$		
C(3)–C(4)	1.443(8)	1.43(2)	C–C–$C_{Ring\ C}$		
C(4)–C(5)	1.344(8)	1.3(1)	O(2)–C(1)–C(2)	108.3(5)	108[a]
C(4)–O(2)	1.431(7)	1.38(2)	C(3)–C(2)–C(1)	108.5(6)	No hits
C(5)–C(13)	1.449(7)	1.47(2)	C(2)–C(3)–C(4)	109.7(6)	No hits
C(6)–C(7)	1.504(9)	1.51(2)	O(2)–C(4)–C(3)	105.4(5)	107.8(5)
C(13)–C(14)	1.406(7)	1.41(2)	C(4)–C(5)–C(13)	136.4(5)	No hits
C(13)–C(18)	1.421(8)	1.41(2)	C(7)–C(6)–C(2)	112.4(5)	113(3)
C(14)–C(15)	1.394(8)	1.38(2)	C(14)–C(13)–C(5)	127.2(5)	121(3)
C(15)–C(16)	1.391(8)	1.38(2)	C(18)–C(13)–C(5)	116.4(5)	121(3)
C(16)–C(17)	1.376(8)	1.38(2)	C(1)–O(2)–C(4)	108.1(4)	107(1)
C(17)–C(18)	1.395(8)	1.38(2)	C(18)–O(5)–C(21)	118.7(5)	118(2)
C(14)–O(3)	1.351(6)	1.37(2)	C(14)–O(3)–C(19)	119.4(4)	118(2)
C(16)–O(4)	1.357(7)	1.37(3)	C(16)–O(4)–C(20)	118.7(5)	118(3)
C(21)–O(5)	1.422(7)	1.42(4)	C–C–$C_{Ring\ B(mean\ value)}$	120.0(4)	120(2)
C(18)–O(5)	1.358(7)	1.38(2)	C–C–$C_{Ring\ C(mean\ value)}$	120(2)	120(3)

[a] One hit appeared in the MOGUL intra-molecular analysis.

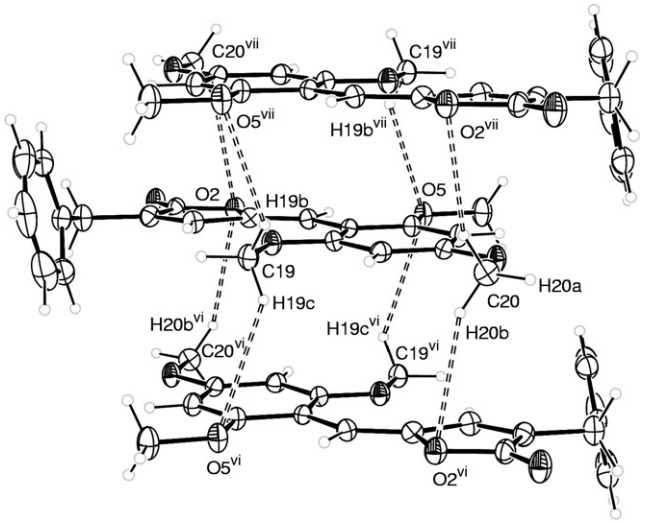

Fig. 9. View of the network of hydrogen bonds parallel to [10-1] for compound (**5**). *Symmetry codes*: vi = $-x+2$, $-y$, $-z+1$; vii = $-x+1$, $-y$, $-z+1$.

or thermodynamic in origin, we performed density functional theory calculations (B3LYP/6-31+G* level) (Fig. 10) using the Gaussian03 program. After convergence, the differences in energy between the two geometric isomers (**4*Z*** & **4*E***) and (**5*Z*** & **5*E***) in the gas phase were 14.18 and 0.96 kJmol^{-1} respectively, with the crystal structures **4*Z*** and **5*E*** having the lowest energies. Thus the fact that isomers **4*Z*** and **5*E*** are found within the solid state is not the result of crystal packing forces or intermolecular bonding motifs depicted in Figs. 4 and 7, but rather is due to these two structures being the lowest energy forms. The transition states of the reactions involving formation of (**4**) and (**5**) probably predispose formation of these geometric isomers and the isomer selection forces appear to be thermodynamic rather than kinetic in origin. For instance, the hydrogen bond seen in (**5**) is probably a result of a destabilizing interaction (steric repulsion between O5 and O2). Also, the hydrogen bonding motif detected between O3 and H3 which may arise in the transition state in a Michael type association preselects the geometry into the observed form (Fig. 7). The structure of nostoclide I which has the *Z* configuration has been determined by single crystal X-ray diffraction [11]. In this case the presence of the isopropyl group precludes adoption of the *E* form.

4. Conclusion

In this study, we fully characterise two nostoclide analogues, and using a variety of structural and spectroscopic methods, verify compound identity. In addition, the correlation between spectral properties and the observed geometries using X-ray diffraction will aid analysis of new compounds and, importantly, aid future exploration of structure activity relationships for ascertaining the nostoclide pharmacophore and the binding requirements of the receptor.

5. Supplementary material

Supplementary crystallographic data sets for (**4**) and (**5**) are available through the Cambridge Structural Data Base,

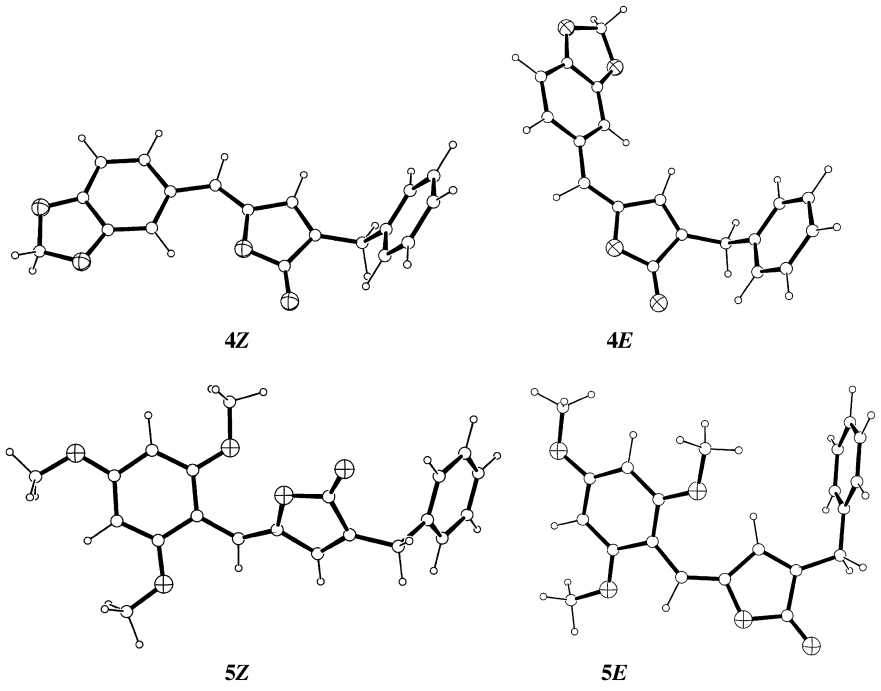

Fig. 10. Energies in atomic units for conformers of **4*Z***: −1033.36053; **4*E***: −1033.35512; **5*Z***: −1188.39793; **5*E***: −1188.39829. Structure **4*Z*** and **5*E*** correspond to conformations found within crystal structures. Large hashed circles, oxygen; medium circles, carbon, small circles, hydrogen.

deposition numbers CCDC 619585 and 619586, respectively. Copies of this information may be obtained free of charge from The Director, CCDC, 12 Union Road, Cambridge, CB2 1EZ, UK (Fax: +44 123 336 033; e-mail: deposit@ccdc.cam.ac.uk or http:www.ccdc.ac.uk).

Acknowledgements

We thank the Brazilian Research Council CNPq (Conselho Nacional de Desenvolvimento Científico e Tecnológico) for research fellowships (LCAB, DPV, RRT), and FAPEMIG (Fundação de Amparo à Pesquisa do Estado de Minas Gerais) for financial support. One of us, A.C.D., thanks the Instituto Rocasolano-CSIC, Spain, for the CSD licence.

References

[1] J. Stetter, F. Lieb, Angew. Chem. Int. Ed. 39 (2000) 1724.
[2] C. Tomlin (Ed.), The Pesticide Manual, Royal Society of Chemistry, Cambridge, 1994.
[3] M.D. Devine, A. Shukla, Crop Protection 19 (2000) 881–889.
[4] (a) A.J. Demuner, L.C.A. Barbosa, T.A.M. Veiga, R.W. Barreto, B.K. Diaz, B.L. Hennssen, Biochemical Systematics and Ecology 34 (2006) 790–795;
(b) L.C.A. Barbosa, A.V. Costa, D.P. Veloso, J.L.C. Lopes, M.G. Hernandez-terrones, B.K. Diaz, B.L. Hennsen, Z. Naturforschung 59c (2004) 803;
(c) L.C.A. Barbosa, M.L. Ferreira, A.J. Demuner, A.A. Silva, R.C. Pereira, Quím. Nova 24 (2001) 1;
(d) L.C.A. Barbosa, E.S. Alvarenga, A.J. Demuner, L.S. Virtuoso, A.A. Silva, Chem. Biodiversity 3 (2006) 553.
[5] (a) J.R. Vyvyan, Tetrahedron 58 (2002) 1631;
(b) S.O. Duke, F.E. Dayan, J.G. Romagni, A.M. Rimando, Weed Res. 40 (2000) 49;
(c) S.O. Duke, J.A. Romagni, F.E. Dayan, Crop Protection 19 (2000) 583;
(d) S.O. Duke, F.E. Dayan, A.M. Rimando, K.K. Schrader, G. Aliotta, A. Oliva, J.G. Romagni, Weed Sci. 50 (2002) 138;
(e) S.O. Duke, in: J.M. Clark, H. Ohkawa (Eds.), New Discoveries in Agrochemicals, ACS Symposium Series 892, 2005, Chap. 14, p. 151.
[6] J.J. Pignatello, J. Porwooll, R.E. Carlson, A. Xavier, F.K. Gleason, J. Org. Chem. 48 (1983) 4035.
[7] F.K. Gleason, C.A. Baxa, FEMS Microbiol. Lett. 33 (1986) 85.
[8] F.K. Gleason, D.E. Case, Plant Physiol. 80 (1986) 834.
[9] F.K. Gleason, J.L. Paulson, Arch. Microbiol. 138 (1984) 273.
[10] F.K. Gleason, FEMS Microbiol. Lett. 68 (1990) 77.
[11] X. Yang, Y. Shimizu, J.R. Steiner, J. Clardy, Tetrahedron Lett. 34 (1993) 761.
[12] (a) G.W. Gribble, Pure Appl. Chem. 68 (1996) 1699;
(b) G.W. Gribble, Chemosphere 52 (2003) 289;
(c) F.M.D. Ismail, J. Fluorine Chem. 118 (2002) 27.
[13] (a) L.C.A. Barbosa, C.R.A. Maltha, A.J. Demuner, F.R. Gann, A.A. Silva, Quím. Nova 28 (2005) 444;
(b) L.C.A. Barbosa, C.R.A. Maltha, A.J. Demuner, C. Filomeno, A.A. Silva, Quím. Nova 27 (2004) 241;
(c) L.S. Lima, L.C.A. Barbosa, E.S. Alvarenga, A.J. Demuner, A.A. Silva, Aust. J. Chem. 36 (2003) 625;
(d) L.C.A. Barbosa, E.S. Alvarenga, A.J. Demuner, R. Figueiredo, A.A. Silva, Pest. Manag. Sci. 59 (2003) 1043;
(e) L.C.A. Barbosa, A.V. Costa, A.J. Demuner, A.A. Silva, J. Agric. Food Chem. 47 (2000) 4807;
(f) L.C.A. Barbosa, J. Braz. Chem. Soc. 8 (1997) 19.
[14] Enraf-Nonius *COLLECT*. Nonius BV, Delft, The Netherlands, 1997–2000.
[15] Z. Otwinowski, W. Minor, in: C.W. CarterJr., R.M. Sweet (Eds.), Methods in Enzymology, vol. 276, Academic Press, New York, 1997, p. 307.
[16] G.M. Sheldrick, *SHELXS-97*. Program for Crystal Structure Resolution, University of Göttingen, Göttingen, Germany, 1997.
[17] G.M. Sheldrick, *SHELXL-97*. Program for Crystal Structures Analysis, University of Göttingen, Göttingen, Germany, 1997.
[18] L.J. Farrugia, J. Appl. Cryst. 32 (1999) 837.
[19] F.H. Allen, O. Johnson, G.P. Shields, B.R. Smith, M. Towler, J. Appl. Cryst. 37 (2004) 335.
[20] I.J. Bruno, J.C. Cole, P.R. Edgington, M.K. Kessler, C.F. Macrae, P. McCabe, J. Pearson, R. Taylor, Acta Crystallogr. B58 (2002) 389.
[21] L.J.J. Farrugia, Appl. Cryst. 30 (1997) 565.
[22] Cerius 2 software, Accelerys Inc., San Diego, CA, USA.
[23] M.J. Frisch, G.W. Trucks, H.B. Schlegel, G.E. Scuseria, M.A. Robb, J.R. Cheeseman, V.G. Zakrzewski, J.A. Montgomery, R.E. Stratmann, J.C. Burant, S. Dapprich, J.M. Millam, A.D. Daniels, K.N. Kudin, M.C. Strain, O. Farkas, J. Tomasi, V. Barone, M. Cossi, R. Cammi, B. Mennucci, C. Pomelli, C. Adamo, S. Clifford, J. Ochterski, G.A. Petersson, P.Y. Ayala, Q. Cui, K. Morokuma, D.K. Malick, A.D. Rabuck, K. Raghavachari, J.B. Foresman, J. Cioslowski, J.V. Ortiz, B.B. Stefanov, G. Liu, A. Liashenko, P. Piskorz, I. Komaromi, R. Gomperts, R.L. Martin, D.J. Fox, T. Keith, M.A. Al-Laham, C.Y. Peng, A. Nanayakkara, C. Gonzalez, M. Challacombe, P.M.W. Gill, B. Johnson, W. Chen, M.W. Wong, J.L. Andres, M. Head-Gordon, E.S. Replogle, J.A. Pople, GAUSSIAN98 program, Gaussian Inc., Pittsburgh, PA, 1998.
[24] (a) G. Casiraghi, F. Zanardi, G. Appendino, G. Rassu, Chem. Rev. 100 (2000) 1929;
(b) J. Boukouvalas, F. Maltais, N. Lachance, Tetrahedron Lett. 35 (1994) 7897;
(c) J. Boukouvalas, N. Lachance, M. Ouellete, M. Trudeau, Tetrahedron Lett. 39 (1998) 76665;
(d) A. Kar, S. Gogoi, N.P. Argade, Tetrahedron 61 (2005) 5297;
(e) F. Bellina, C. Anselmi, S. Viel, L. Mannina, R. Rossi, Tetrahedron 57 (2001) 9997;
(f) F. Bellina, C. Anselmi, R. Rossi, Tetrahedron Lett. 43 (2002) 2023;
(g) L.C.A. Barbosa, A.J. Demuner, E.S. de Alvarenga, A. Oliveira, B.K. Diaz, B.L. Hennsen, Pest. Manag. Sci. 62 (2006) 214.
[25] I.J. Bruno, J.C. Cole, M. Kessler, J. Luo, W.D.S. Motherwell, L.H. Purkis, B.R. Smith, R. Taylor, R.I. Cooper, S.E. Harris, A.G. Orpen, J. Chem. Inf. Comput. Sci. 44 (2004) 2133.
[26] F.H. Allen, Acta Crystallogr. B58 (2002) 380.